Laboratory Experiments of Polarimetric Radar Interferometry: DEM Generation and Vegetation Height Estimation

J. M. Lopez-Sanchez[1], L. Sagués[2], J. Fortuny[1], X. Fàbregas[2], A. Broquetas[2], A. J. Sieber[1] and S. R. Cloude[3]

[1] Space Applications Institute, JRC, 21020 Ispra (Va), Italy
Phone/Fax: +39 0332 785104/5469, E-mail: juan.lopez-sanchez@jrc.it

[2] Universitat Politècnica de Catalunya (UPC), Campus Nord, c/ Jordi Girona, 1-3, 08034 Barcelona, Spain
Phone/Fax: +34 93 4011065/7232, E-mail: sagues@voltor.upc.es

[3] Applied Electromagnetics, 11 Bell St, St.Andrews KY16 9UR, United Kingdom
Phone/Fax: +44 1334 477598/5570, E-mail: scloude@fges.demon.co.uk

Abstract - A coherence optimization method, which makes use of polarimetry to enhance the quality of the interferograms, has been experimentally tested under laboratory conditions in an anechoic chamber. The experiments have proved the remarkable contribution that this technique offers in two important applications: the improvement of Digital Elevation Maps (DEM) generation and the estimation of the height of vegetation targets.

INTRODUCTION

An important application of Radar Interferometry is the extraction of high resolution DEM's of terrain. The quality of the interferograms depends on the correlation (coherence) between the two complex SAR images. If a high signal-to-noise ratio is assumed and there is no temporal decorrelation, then the most important source of decorrelation is that produced by the separation between the two antennas (spatial baseline decorrelation). The difference between the two viewing angles produces a shift and a stretch of the two imaged terrain spectra that can be compensated by shifting the transmitted center frequency during the second measurement or by removing the disjoint parts of both spectra [1]. However, the different height of the scattering centers inside the resolution cell (volumetric effects) [2] is an important source of spectral decorrelation which can not be compensated by filtering the two spectra since they have different shapes. If fully polarimetric interferometric data are collected, a coherence optimization can be performed by expressing the obtained SAR images in arbitrary polarization bases (what is equivalent to select arbitrary scattering mechanisms) that maximize the interferometric coherence [3]. The proposed coherence optimization has been experimentally tested in the anechoic chamber of the European Microwave Signature Laboratory (EMSL) at JRC Ispra [4].

COHERENCE OPTIMIZATION

When fully coherent polarimetric backscatter data are collected in the usual (H,V) basis, we can easily apply a first optimization by extracting the interferometric phase which is associated to the polarization combination that maximizes the interferometric coherence. However, the interferograms can be formed by using not only linear polarization states but also any other combination between arbitrary elliptical polarization states. These elliptical polarization states can be generated by applying a change of basis from (H,V) to in any other orthogonal basis [5]. Physically, this transformation can be interpreted as a change of the selected scattering mechanisms in both images. The application of these basis transformations allows us to form interferograms between all possible elliptical polarization states and combinations between both SAR images, and the best interferometric phase estimation will be given by selecting that combination which maximizes the coherence. This optimization problem has been solved in [3] by introducing a vector formulation into the interferometric coherence definition. The optimization leads to two 3×3 complex eigenvalue problems. The eigenvalues are real and the optimum coherence will be given by the highest one. The interferometric phase associated to the optimum scattering mechanisms will be used in the experiments to generate the DEM of non vegetated surfaces. In addition, the eigenvalue solution yields other two pairs of scattering mechanisms corresponding to the second and third eigenvalues. If the target consists of some layers with different physical components, placed at different heights, it can be equivalently modeled by different scattering mechanisms at different heights. In this case, the second and third pair of optimum scattering mechanisms should be associated to the phase centers of these layers and, therefore, additional interferograms can be computed giving the height of these layers. An application of this processing is the estimation of the height of vegetation, since most plants can be modeled by this multilayer morphology.

EXPERIMENTAL RESULTS

In the first experiment, a 2×2 m planar rough surface of gravel has been measured. A series of fully polarimetric strip-map SAR data sets have been acquired in the frequency range 8 to 12 GHz, with 9 uniformly spaced viewing angles ranging from 43° to 47° (thus having angular baselines from 0.5° up to 4°). The experimental setup of the measurement is shown

Lluís Sagués thanks the CICYT (Spanish Commission for Science and Technology) for the financial support of his three-month stage at JRC

0-7803-5207-6/99/$10.00 © 1999 IEEE.

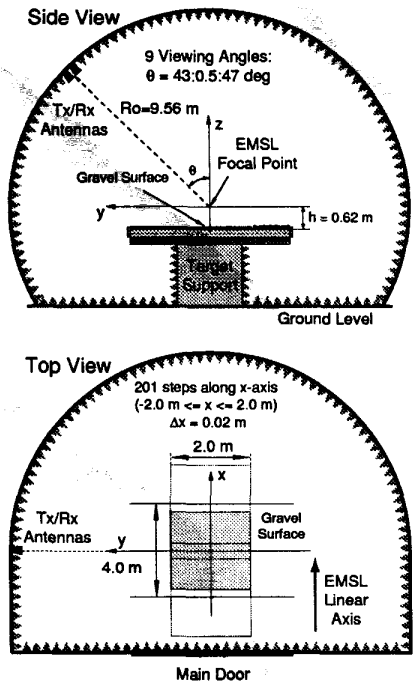

Figure 1: Experimental set-up. The synthetic aperture length is 4 m, and the cross-range and ground-range resolutions are approximately 4 cm

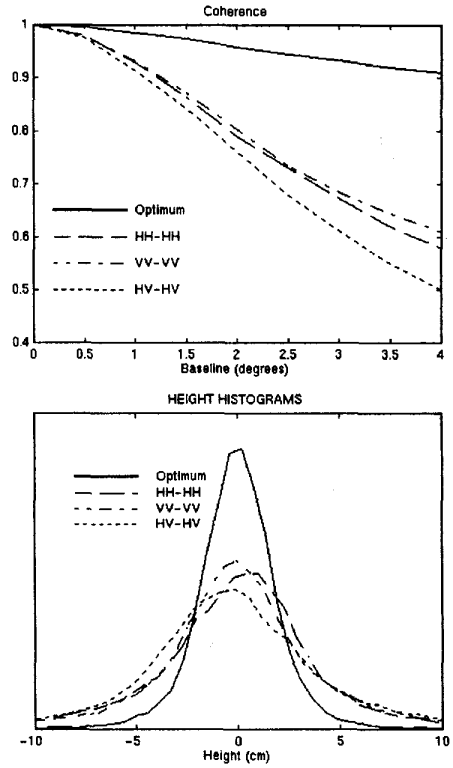

Figure 2: Mean coherence vs baseline (top), and height error histogram at $B = 1°$ (bottom) for the planar rough surface

in Fig. 1. With such a measurement geometry, the near-field phase distortion can be accounted for by considering a spherical wavefront illuminating the target. The 2D complex reflectivity images for each polarization have been reconstructed on a horizontal plane using a near-field SAR processor especially suited for the EMSL geometry [6].

As shown in Fig. 2 for the planar rough terrain, the interferometric coherence is importantly degraded as the baseline increases when using copolarized data. However, the coherence is near to one for all baselines after applying the polarimetric optimization process. Then, it is possible to use longer baseline distances for improving the height accuracy while keeping the coherence high. Fig. 2 also shows the mean squared height error histograms obtained for a specific baseline $B = 1°$.

A small mountain was also built using the same gravel surface. The maximum height of this mountain was 12 cm and it was located at the middle of the surface. Fig. 3 shows a comparison between the elevation map that was generated using two copolarized HH-HH images and that obtained after applying the polarimetric optimization algorithm. The HH-HH elevation map presents some noisy zones where the height error is very high and therefore the mountain can not be clearly distinguished. This height error is mainly produced by the baseline distance (spatial baseline decorrelation) and the random height distribution of the scatterers inside the resolution cell (volumetric effects). After applying the coherence optimization algorithm the noisy zones are removed and the obtained elevation map reproduces the actual profile of the measured surface: the top of the mountain appears at its real position and the shape of the mountain is well reconstructed. The obtained mean coherence values and the squared mean height error are also described in Table I.

The second part of the experiment is the validation of the retrieval algorithm for vegetation height presented in [3]. The target (see photograph in Fig. 4) is a stand of 6×6 young plants of maize about 1.8 m high, uniformly planted on a square container with side length 2 m. As explained in [7], this target can be modeled by a single layer of random scatterers over the ground. The random layer occupies a height of about 1.4 m and is 0.4 m above the ground. Therefore, assuming that the dominant scattering mechanisms are associated to the random layer and the ground (or ground-trunk interaction) the expected height to be estimated is about 1.1 m, which is the distance between the center of the random volume and the ground. A fully

Table I: Coherence and height error for $B = 1°$ (mountain)

Pol. Combination	Mean Coherence	Height error (cm)
HH-HH	0.8898	4.85
HV-HV	0.8851	6.49
VV-VV	0.8831	5.62
Optimum	0.9568	2.87

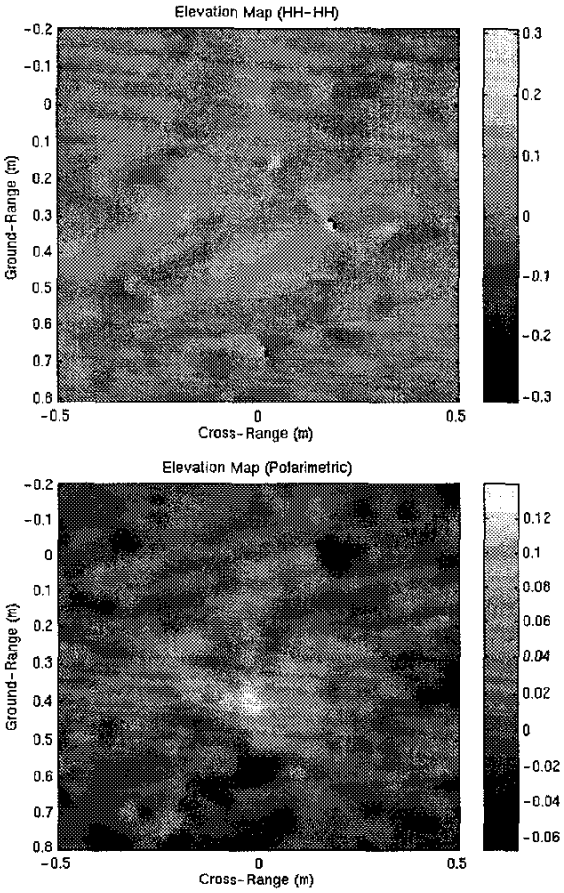

Figure 3: Elevation maps corresponding to a gravel small mountain ($B = 1°$). Top: HH-HH channels. Bottom: Optimum

polarimetric measurement was carried out in the band 1.5 to 9.5 GHz. The elevation incidence angle ranged from 44° to 45° with a step of 0.25°. The target was rotated in azimuth with a step of 5°, thus obtaining 72 independent samples. Reflectivity images where computed with a narrow bandwidth in order to enclose the whole target inside the resolution cell. The estimation results as a function of the frequency are shown in Fig. 4 for a baseline of 0.25°. Despite the wider spread of estimations for low frequencies than for high frequencies and a slightly decreasing trend, the results confirm the ability of this algorithm for estimating the height of this vegetation sample at this frequency range. To the authors' knowledge, it is the first result of this technique that has been successfully compared with ground truth data, since previous works do not provide a precise description of the structure and true height of the measured vegetation layers [3, 8].

CONCLUSIONS

The obtained results show that the height error in DEM generation can be drastically reduced within a wide range of baselines by using this optimization algorithm. Moreover, the estimated

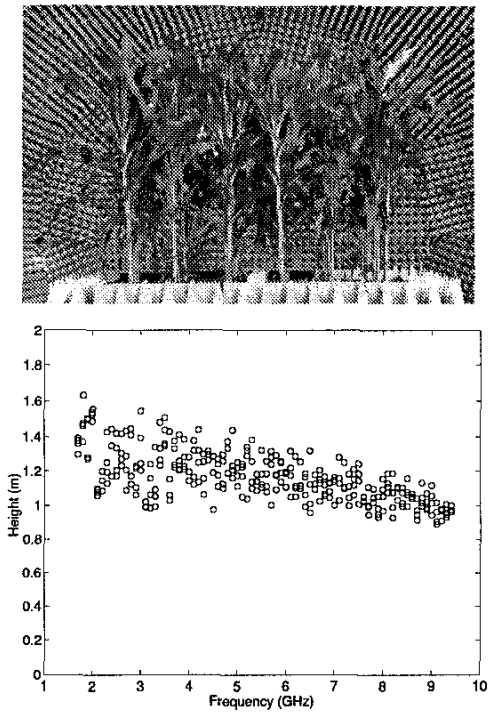

Figure 4: Photograph of the maize sample (top), and height estimations vs frequency (bottom)

height for a maize sample is quite satisfactory, and it is the first example in the literature where a comparison with ground truth data has been done using this technique. There are some aspects that have not been deeply analyzed yet, like the effect of multiple scattering on the retrieved position of the phase centers and the influence of differential extinction coefficient between orthogonal polarizations.

REFERENCES

[1] F. Gatelli *et al*, "The wavenumber shift in SAR interferometry," *IEEE Trans. Geosci. Remote Sensing*, vol. 32, pp. 855–864, July 1994.

[2] L. Sagués, M. Bara, X. Fàbregas, and A. Broquetas, "A study of spectral decorrelation sources in wide band interferometry," in *Proceedings of the PIERS - Workshop on Advances in Radar Methods*, (Baveno, Italy), pp. 64–66, July 1998.

[3] S. R. Cloude and K. P. Papathanassiou, "Polarimetric SAR interferometry," *IEEE Trans. Geosci. Remote Sensing*, vol. 36, pp. 1551–1565, Sept. 1998.

[4] A. J. Sieber, "The European Microwave Signature Laboratory," *EARSel Advances in Remote Sensing*, vol. 2, pp. 1995–204, Jan. 1993.

[5] S. R. Cloude and E. Pottier, "A review of target decomposition theorems in radar polarimetry," *IEEE Trans. Geosci. Remote Sensing*, vol. 34, pp. 498–518, Mar. 1996.

[6] J. Fortuny and A. J. Sieber, "Fast algorithm for a near-field synthetic aperture radar processor," *IEEE Trans. Antennas Propagat.*, vol. 42, pp. 1458–1460, Oct. 1994.

[7] J. M. Lopez-Sanchez, J. Fortuny, S. R. Cloude, and A. J. Sieber, "Indoor polarimetric radar measurements on vegetation samples at L, S, C and X band," *J. Electromag. Waves Appl.*, 1999. In press.

[8] K. P. Papathanassiou and S. R. Cloude, "Phase decomposition in polarimetric SAR interferometry," in *Proceedings of IGARSS*, vol. 4, (Seattle), pp. 2184–2186, July 1998.